University of Dayton
eCommons

Honors Theses | University Honors Program

4-1-2024

Hippo, Wnt, and JNK Pathway Interactions in a Drosophila Colorectal Cancer Model

Michael K. Gruhot
University of Dayton

Follow this and additional works at: https://ecommons.udayton.edu/uhp_theses

eCommons Citation
Gruhot, Michael K., "Hippo, Wnt, and JNK Pathway Interactions in a Drosophila Colorectal Cancer Model" (2024). *Honors Theses*. 440.
https://ecommons.udayton.edu/uhp_theses/440

This Honors Thesis is brought to you for free and open access by the University Honors Program at eCommons. It has been accepted for inclusion in Honors Theses by an authorized administrator of eCommons. For more information, please contact mschlangen1@udayton.edu, ecommons@udayton.edu.

Hippo, Wnt, and JNK Pathway Interactions in a *Drosophila* Colorectal Cancer Model

Honors Thesis

Michael Gruhot

Department: Biology

Advisor: Madhuri Kango-Singh, Ph.D.

April 2024

Hippo, Wnt, and JNK Pathway Interactions in a *Drosophila* Colorectal Cancer Model

Honors Thesis
Michael Gruhot
Department: Biology
Advisor: Madhuri Kango-Singh, Ph.D.
April 2024

Abstract

Colorectal cancer (CRC) will be the leading cause of cancer-related deaths for people under the age of 50 by 2030. Due to increased efforts to spread awareness for regular screenings, the five-year relative survival rate for those diagnosed with colon cancer is 64.4% (www.fightcolorectalcancer.org). Treatment for CRC consists primarily of the excision of the tumor paired with regular doses of chemotherapy and radiation therapy. These treatments cause systemic stress, damaging both cancerous and healthy cells alike. In order to create more efficient treatments, first, we must better understand the biology underlying changes in cells that lead to tumors in the colon. The proposed research aims to generate a better understanding of CRC using genetic models in *Drosophila*. We will specifically study the roles of the Hippo, Wnt, and JNK pathways on tumor formation and metastases in the colon. In order to do this, we have designed one- and three-hit models that disrupt each pathway singly and in combination with each other. These models represent the genetic heterogeneity in cancer patients, as well as represent the three most frequently found genetic lesions (p53, Ras, and APC.). The CRC models in flies will generate patches of cancerous cells in the fly gut (intestine). We will evaluate the CRC models (a) using antibody staining to check pathway activity (JNK, Wg, Hippo) and (b) using antibody staining to determine levels of proliferation and cell death. Overall, our studies will provide a platform for evaluating the effects of the three common genetic lesions in CRC and add to our knowledge about the altered communication between these oncogenes and pathways in CRC.

Acknowledgments

I would like to thank my mentor Dr. Madhuri Kango-Singh for giving me the opportunity to challenge and develop myself these past few years as both a student and researcher. Through her guidance, I have been able to learn much that I know will assist me in the years to come. I would also like to thank Arushi Rai for the immense help that she has provided towards this project. She, along with the rest of the CRC team, has helped to make this project possible. Lastly, I would like to thank the University of Dayton Honors Program for the opportunity to create and present my Honors Thesis in the field that I am passionate about.

Table of Contents

Chapter 1

Introduction

What is colorectal Cancer (CRC)?

On average, a person has a 1 in 20 chance of developing colon cancer over their lifetime, it is the third most common cancer in the United States (www.americancancerfund.org). Besides the prevalence of colon cancer, treatment is often difficult as the progression and the stage of the cancer may vary significantly by the time of diagnosis in patients. Many times, CRC does not present symptoms until it has had time to develop into later stages. These symptoms can also change based on where in the intestine the cancer develops first. The presentation of the cancer does not provide direct insights into the root cause of the disease. For those with colon cancer, treatment can be invasive and uncomfortable. Surgery followed by chemo- and radiotherapy is the standard of care for this cancer.

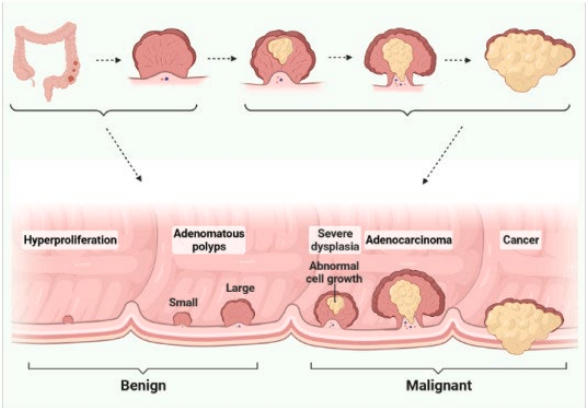

Figure 1: Cartoon depicting the progression of a benign intestinal polyp into a cancerous polyp. As the cell mass moves through the intestinal wall, it becomes malignant.

CRC typically begins with alterations in the epithelial lining of the intestine, where the cells lining the intestine or colon change their shapes, grow uncontrollably, and form clumps of cells called polyps that are more prominent in older adults. While not all polyps are cancerous, some can develop into cancerous tumors known as adenomatous polyps as they develop (Islam et al). This is the reason that early detection is thought to present the opportunity for

effective CRC treatment. According to the CDC, it is recommended that anyone over the age of 45 begins regular screening for the development of these polyps. This includes stool tests, colonoscopy, CT colonography, and flexible sigmoidoscopy (CDC). Patients with other risk factors than age such as family history or inflammatory bowel disease are recommended to get screened younger and more often to ensure early detection.

Genetic alterations associated with Colorectal Cancer

Molecular studies on CRC, like The Cancer Genome Atlas (TCGA), have revealed the genetic and genomic alterations associated with CRC cancers. These and other genomic studies revealed the most frequently altered genes in CRC. Overall, colorectal cancer is associated with two broad types of inherited conditions, the Familial Adenomatous Polyposis (FAP) or the Hereditary Non-Polyposis Colon Cancer (HNPCC). The FAP is caused by mutations in genes involved in development, DNA damage control, or activation of oncogenes. Frequent among these mutations are activating mutations in oncogenes like *Ras*, and loss of tumor suppressor genes like the Wnt pathway gene *Adenomatous Polyposis coli* (*apc*), and *p53* - the guardian of the genome.

Types of CRC	Genes involvement	Chromosomal locus	Inheritance pattern
Sporadic	APC	5q22.2	Non-inherited
	K-RAS	12p12.1	
	DCC	18q21.2	
	P53	17p13.1	
	COX-2	2p14.1	
	BCL-2	18q21.33	
	related MMR genes		
	etc.		
Familial	Unknown	---	Non-inherited
Hereditary			
FAP	APC	5q22.2	AD
MAP	MUTYH	1p34.1	AR
PJS	STK11/ LKB1	19p13.3	AD
SPS	Unknown	---	---
LS	MLH1 MSH2 MSH6 PMS2	3p22.2 2p21-p16.3 2p16.3 7p22.1	AD

Figure 2: Table depicting the most common mutations associated with the development of CRC. (Nouri Nojadeh et al., 2018)

HNPCC, on the other hand, is caused by mutations associated with mismatch repair genes (a pathway meant to control errors during DNA replication) (ref). In our lab,

we are interested in understanding the mechanisms that drive the growth of FAP. Due to the high rate of mutations in genes observed in human patients (Figure 2), we decided to use these in our fly CRC models.

Cooperative Oncogenesis in Cancer and CRC

The interaction between these different pathways is essential to understanding the process behind tumor formation and the conversion of normal cells to benign tumors, and then to malignant ones. The combination of mutations in both tumor suppressor genes and proto-oncogenes is often associated with aggressive tumors with poor prognosis. Such cooperative oncogenic interactions are well-known in several cancers (Delaval and Birnbaum, 2007; Dillard et al., 2021; Richardson et al., 2020; Yasuta et al., 2024). A hallmark study of the cooperative oncogenesis in *Drosophila* (Fig. 3) shows the effects of combining oncogenic Ras (*UAS-Ras*^{V12}) and the tumor suppressor gene *scribble* (Dillard et al., 2021). Individual mutations in either of these genes produce clones that result in benign tumors (Fig. 1 B, C). It is when the two mutations are combined that we see malignant tumors form (Fig. 1 D) (Dillard et al., 2021, Snigdha et al., 2019). This cooperation can be seen in CRC through the development of larger, more aggressive tumors. Polyps that grow as the result of a single mutation will develop slower if at all due to the cell's natural defenses against malignant DNA mutations. Oncogenes are the mutated variants of genes responsible for the proliferation and differentiation of cells. Once mutated, they provide protein signals for the cell to undergo constant division regardless of environment, leading to the development of tumors. Tumor suppressor genes catch and prevent many mutations such as these from developing into fully

cancerous cells. It is when a mutation occurs in both types of genes that most cancers are able to develop.

Roles of the Signaling Pathways

Signaling pathways exist in cells where a group of molecules work together to control several cell biological and developmental processes, such as the proliferation. Aberrant signaling or excessive signaling due to genetic alterations results in unregulated cell growth and other changes in cellular behaviors such as invasion, that we see present in cancerous cells (Sanchez-Vega et al., 2018). Mutation in the oncogenic Ras (*UAS Ras*^{V12}) gene is linked to the disruption of both the JNK and Hippo pathways (Waghmare et al., 2023). The main function of the Hippo pathway is to limit organ size through the control of cell proliferation (Kango-Singh and Singh, 2009). This pathway comprises two serine-threonine kinases, Hippo (Hpo) and Warts (Wts). When the pathway is turned on, Hpo and its adaptor protein Salvador phosphorylates and activates Wts. Wts and its cognate adaptor Mats, inactivate the transcriptional co-factor Yorkie (Yki) through phosphorylation. Phosphorylated Yki is destined for proteasomal degradation (Kango-Singh and Singh, 2009). Downregulation of the Hippo pathway results in the relief of Wts-mediated Yki repression allowing it to function as a transcriptional co-activator. Thus, unphosphorylated Yki protein

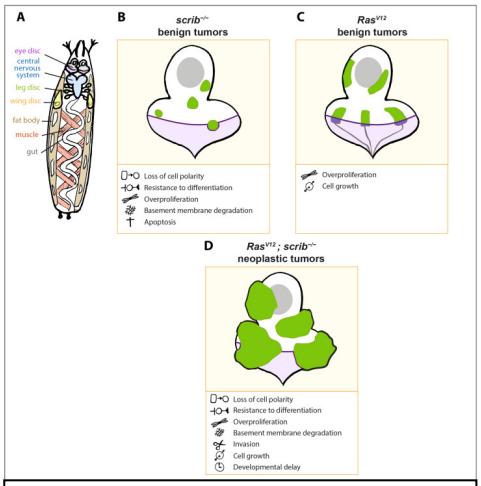

Figure 3: Cartoon depicting cooperative oncogenesis in Drosophila tissues. The panels depict effects of Ras activation and loss of tumor suppressor genes individually (B,C) and their cooperative interactions (D).

translocates to the nucleus where it binds the transcription factors like Scalloped (Sd), Homothorax (Hth), or Teashirt (Tsh), and regulates the expression of target genes to control cell proliferation and cell survival. The Hippo pathway controls the expression of these genes by regulating the amount of nuclear Yki (Doggett et al., 2011). In the context of tumor growth, regeneration, cell competition, and stress response, the Hippo pathway is also linked to the Jun N-terminal kinase (JNK) pathway (La Marca and Richardson, 2020, Sun and Irvine, 2011, Igaki et al., 2006).

The JNK pathway plays an important role in both apoptosis and cell proliferation and is activated in response to stress or oncogenic signals (La Marca and Richardson, 2020). JNK is known to act in a context-dependent manner, where it can induce apoptosis of the cell, and also simultaneously signal for compensatory cell proliferation from neighboring cells through the reactivation of Yki (Sun and Irvine, 2011).

Mutations in an additional pathway known as the Wingless (Wnt) pathway appear in almost all cases of colorectal cancer. This pathway is activated when WNT ligands bind to Frizzled and LRP receptor complexes. This disables the β-catenin destruction complex composed of APC, axis inhibition protein 1 (AXIN1), casein kinase 1 (CK1), and glycogen synthase kinase-3 beta (GSK3β). The disabling of these destruction complexes allows for β-catenin to build up within the cell and promote the transcription of genes that cause cell proliferation (Bejsovec, 2018). When there is a mutation in this pathway, cell proliferation becomes unregulated allowing for uncontrolled growth as seen in tumors (Schatoff et al., 2017). Further mutations in the *p53* gene, the guardian of the genome, can lead to the activation of β-catenin-dependent transcription factors, subverting this pathway and triggering cell proliferation (Nakayama and Oshima, 2019).

Fly to Human Correlation

The use of *Drosophila* for the study of genetics and diseases like cancer has been invaluable (Waghmare et al., 2014; Mirzoyan et al., 2019; Snigdha et al., 2019). They provide an opportunity to study first-hand the effects of mutations in key proteins on cell signaling pathways as well as ways to increase our understanding of these concepts as a whole (Johnson and Cagan, 2010). *Drosophila* is an extremely powerful model, given the versatility of genetic tools available and the nature of *Drosophila* themselves. These organisms possess the ability to rapidly produce large populations due to a short generation time of ~15 days. During their life cycle, they progress through easily identifiable stages allowing for accurate tracking of the period of development (Fig. 4). Due to their relatively small number of chromosomes and the wide body of research working with these organisms, models can be more easily created to study genetics (Jennings, 2011). Additionally, growth factors and signaling pathways (and cell biological processes like cell division or cell death) are highly conserved between flies and humans. This allows the extrapolation of findings from experiments done using *Drosophila* to mammalian models including humans (Brumby and Richardson, 2005) (Snigdha et al., 2019)(Johnson and Cagan, 2010). Taking advantage of the genetic and functional conservation of genes, we

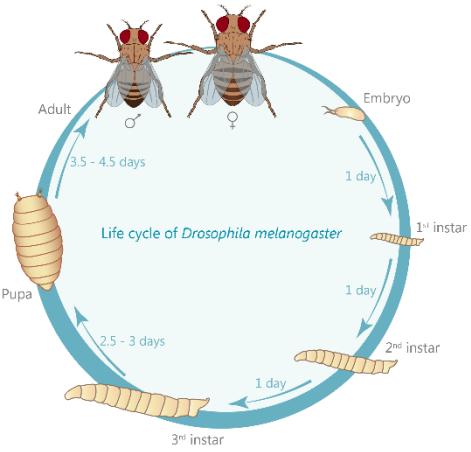

Figure 4: This cartoon depicts the stages of the life cycle of *Drosophila melanogaster*. Samples for this study were collected from the "3rd Instar" stage.

generated a complex CRC model in flies. We combined activation of oncogenic Ras ($UASRas^{V12}$) with loss of both isoforms of APC ($apc2^{N175K}$, $apc1^{Q8}$) and the dominant-negative form of p53 ($UASp53^{H159N}$). Abnormal expression and regulation of these genes lead to altered signaling and induce uncontrolled proliferation of cells in the fly intestine (Armaghany et al., 2012). Characterization of these genetic alterations in *Drosophila* models is expected to generate a better understanding of the influence of these genes and their pathways on both each other and the resulting tumor. We take advantage of genetic tools available in flies to express these genes specifically in the intestinal stem cells for a short period of time (using temperature shift and heat shock strategies) to induce tumors. This allows for the study of the effects of Ras activation, loss of *apc1* and *apc2*, and dominant-negative *p53* on the Hippo, JNK, and Wnt pathways on the development of colorectal cancer in fly intestines. Using a one- and three-hit CRC model, we can better understand the ways in

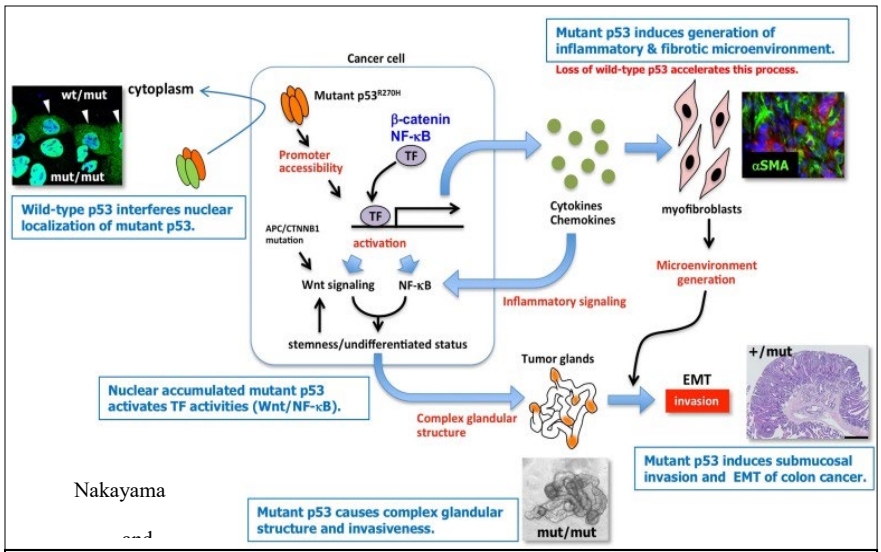

Figure 5: This figure depicts the interactions between *p53* and APC. At the center of the cartoon is a cancer cell that depicts multiple interactions through *p53*. In cancer cells, *p53* enters into the nucleus and causes changes in gene expression leading to increased inflammation in the microenvironment (top right) and altered transcription by interaction with Wnt pathway ultimately resulting in increased metastasis (bottom right).

which these pathways work with each other in tumorigenesis. For the completion of this work, we (1) established a three-hit model with appropriate controls in flies, and (2) evaluated expression levels of JNK, Wnt, and Hippo pathways, and their requirement in intestinal tumors.

Evaluating JNK, Wnt, and Hippo pathways to study intercellular signaling in intestinal tumors

We hope to learn more about the interaction between these individual pathways to explore cooperative oncogenesis in the CRC model. To do so, we will first survey if the target genes of each pathway are induced in the three-hit model and compare the expression profile to our one-hit models to determine which pathway (input) may be responsible for the observed expression profile. A comparison of target genes from each pathway (DIAP for Hippo, Wg for Wnt, and MMP1 for JNK) will help understand the pathway activity and relationships.

Temperature shift method for generating tumors

Three days after fertilized eggs are laid, the vials were placed into a 29ºC incubator for a 24-hour period to allow for gene expression. The next day, all samples are placed in a 25ºC incubator, until mature third instar larvae develop. The intestine are dissected from the larva and rested in a solution of PBS and 4% PFA for 20 minutes. Afterward, the samples are washed with PBST. The primary antibody, mouse anti-Prospero, is added to the samples and they are incubated overnight at 4ºC. After washing 3X PBST for 20 minutes, the sample is incubated in the secondary antibody (anti-mouse Cy3), covered with foil, and nutated for two hours. Next, the samples are washed to

remove unbound secondary antibodies and mounted using Vectashield. The slides are imaged using Olympus Fluoview 3000 Laser Scanning Confocal Microscope. All images are processed using Adobe Photoshop and Quantification was done using Excel or GraphPad Prism 8.0.

Hypothesis

The development and proliferation of cancerous cells are rarely the result of a single mutation due to the safeguards built into cell biology to prevent the unregulated division of cells. In normal functioning cells, these safeguards include systems such as checkpoints in the various stages of cell division and maturation to check for DNA damage, growth inhibition due to crowding of neighboring cells, and the synthesis and degradation of signaling proteins. CRC is the result of failure in these safeguards that lead to the proliferation of cells with damaged DNA, with more damage allowing for less regulation. **My hypothesis** is that our three-hit model will produce larger, more frequent, and more lethal CRC tumors than in any of the individual one-hit models due to the effect of cooperative oncogenesis in tumor formation.

Chapter 2

Materials and Methods

To begin this research, we first needed to create our single- and triple-hit models to show the effect of the Hippo, Wnt, and JNK pathways in tumor oncogenesis. GFP was used as a control between all models to verify the presence of tumor formation in samples. Our single-hit models were created through the knock-out of one of three genes encoding a key protein in each of these pathways. The three genes targeted encoded for DIAP for Hippo, Wg for Wnt, and MMP1 for JNK.

Temperature-shift versus heat-shock induced tumors: Initially, all three of the single-hit models were controlled via a temperature shift system to limit the amount of time tumor formation was promoted in order to prevent hyper-lethal tumor formation killing the models before they had developed appropriately for dissection. This was possible through the UAS/Gal4 system (Brand and Perrimon, 1993). In this system, the transcription factor Gal4 binds to the upstream activation sequence (UAS) of the target gene, promoting transcription. Control of this promotion is done through the use of a temperature-sensitive variant of Gal80, an antagonist of Gal4 (Caygill and Brand, 2016). At room temperature, no transcription of the target gene occurs due to the presence of Gal80, but moving the model to 29ºC incubator destabilizes Gal80, allowing for Gal4 to bind to the UAS (McGuire et al., 2004). This system was used to regulate the expression of the three cancerous variants of key pathways proteins used in our models, *UAS* Ras^{V12}, *UASp53*^{DN}, and *FRT82B* $apc2^{N175K}$ $apc1^{Q8}$ (referred to as *ap2, apc1* in the sections that follow). In order to generate these single-hit models, flies from *yw; escGal4 UASGFP;*

FRT82B Gal80^{ts} will be crossed to *UASp53^{DN}* or *UASRas^{V12}* or *FRT82B apc2, apc1* mutant flies. However, due to concern that tumors grown using this method were too lethal for proper procedure, the *UAS Ras^{V12}* and a*pc2 apc1* crosses were moved to a heat shock method of control instead.

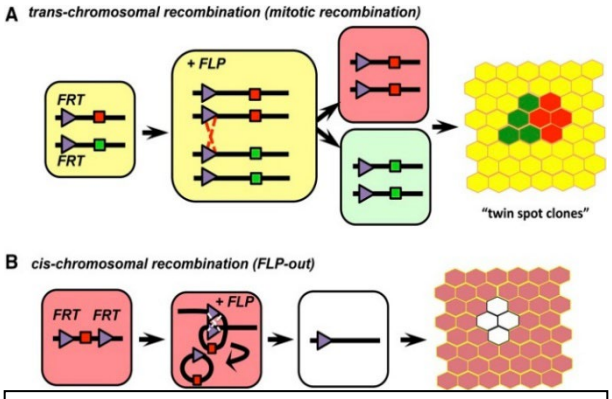

Figure 6: This cartoon depicts the mechanism and results of the FLP/FRT tool for gene expression. Path A shows the mechanism between FRT sites on sister chromatids. Path B shows the mechanism between FRT sites on the same chromosome. In both pathways, FLP promotes recombination between the two FRT sites to generate cells lines with unique genotypes.

Heat-shock mediated 'FLP out' clones: In this method, *FLP recombinase target sites (FRT)* produce mosaic clones that are generated due to the recombination of sister chromatids at the FRT sites. FRT activity is controlled by using a variant, *hsp70p*, that operates at higher temperatures. Similar to the UAS/Gal4 method, this allows for precise control of target gene expression, though this method allows us to decrease the duration of expression to reduce tumor lethality. In order to generate these single-hit models, a *yw hsFLP; escGal4UASGFP; FRT82B TubGal80* will be crossed to *UASp53^{DN}* or *UASRas^{V12}* or <*apc2, apc1* mutant flies.

Once the single-hit models were established, the three-hit model was generated as well. In order to create this model we used the MARCM system, which allows for testing oncogenic cooperation in flies (Lee and Luo, 1999). The system allows simultaneous expression or knockdown of several genes and can be tracked by a cellular marker like GFP (del Valle Rodríguez et al., 2011). We generated the following flies: (Line 1) the

driver line (yw *hsFLP; escGal4UASGFP; FRT82BGal80*), and (line 2) the three-hit line (*yw UASp53DN; UASRas^{V12}, FRT82B apc2, apc1*). When crossed together and administered a heat-shock (20min at 37ºC) the resulting F1 larvae will show small patches of GFP-positive tumors in the fly intestine. The one-hit models will serve as controls for the three-hit model, in which we will assess changes in cell proliferation (PH3), cell survival (DIAP1), and invasion (Laminin) to track changes in protein expression. These studies will help establish multiple CRC models in flies, and complete an initial survey of how different components of the CRC models affect tumor growth and progression.

A strict procedure was followed in order to mitigate as much as possible outside factors and to ensure valid and reliable results. Crosses would be established in a tube with food on day 0. The adult flies (parents) would then be transferred into new tubes daily to easily keep track of the age of the F1 generation in each tube. On day 3, around when the *Drosophila* were 1st instar, they would be subjected to heat treatment to promote cancerous gene expression and oncogenesis along the colorectal tract. This gave the cancerous cells enough time to proliferate, but not long enough to become lethal to the *Drosophila.* These tubes would then be allowed to grow until they reached the 3rd instar stage. At this point, larvae were dissected and the alimentary canal was removed in its entirety.

Immunohistochemistry: Samples dissected from the temperature-shift or hsFLP-based MARCM were then placed into a 1.5ml Eppendorf tube and rested in a solution of 150µL PBS and 50µL PFA 16% for 20 minutes. After resting, 1000µL PBST is added to the Eppendorf tubes, and the samples are set to nutate for 15 minutes. Once this was

complete, any excess fluid was removed and another 1000µL of PBST was added for a second round of 15 minutes of nutation. This washing method was used to remove unwanted debris from the samples. After the excess fluid was again removed, 20-40µl of a primary antibody was added to the samples depending upon the number of samples per tube. These tubes were then incubated at 4ºC in the fridge for 12-24 hours. The primary antibodies used in this experiment were anti-pJNK (1:250, Cell Signaling) used to mark JNK pathway activity, anti-Wg (1:100, DSHB) used to mark Wingless pathway activity, anti-Yki (1:1500) used to mark Hippo pathway activity, anti-PH3 (1:200, Cell Signaling) used to mark cell division, anti-DIAP1 (1:250, Bruce Hay) used to mark dying cells, and anti-DCp-1 (1:200, Cell Signaling) used to mark dying cells. After the incubation, samples were again washed with two rounds of 1000µL of PBST for 15 minutes each time on the nutator to remove any unbound primary antibody. Once the excess fluid had been removed after the second round, the secondary antibody was added at an equal amount to the primary using either anti-mouse Cy3/Cy5, anti-rat Cy3/Cy5, or anti-rabbit Cy3/Cy5. The Eppendorf tubes were then covered with aluminum foil and nutated for 2 hours. Afterward, the samples were washed twice for 15 min with 1000µL PBST to remove any unbound secondary antibodies. Lastly, the samples were then cleaned and mounted onto microscope slides using Vectashield (Vector Labs) to be viewed and images were taken via Olympus Fluoview 3000 Laser Scanning Confocal Microscope.

Figures and quantification of data: Confocal images were then used to produce figures using Adobe Photoshop CS6. The data were quantified using the histogram and measure functions in Adobe Photoshop and processed in GraphPad Prism for statistical analysis and graphs.

Chapter 3

Results

Results were obtained by first establishing the dissecting and staining procedure listed above to ensure no interference from outside factors. Crosses were confirmed to be working consistently and procedure was adjusted until clones could be produced reliably. The presence of tumors was confirmed via GFP markers, allowing for additional staining to be performed to identify key tumor markers. Samples were treated to the same procedure without staining to establish control samples to verify no interference from outside factors. After verifying both the procedure and controls, the intestines from the *UASRas^{V12}, UASp53^{DN}*, and *FRT82B apc2 apc1* crosses were stained for data collection.

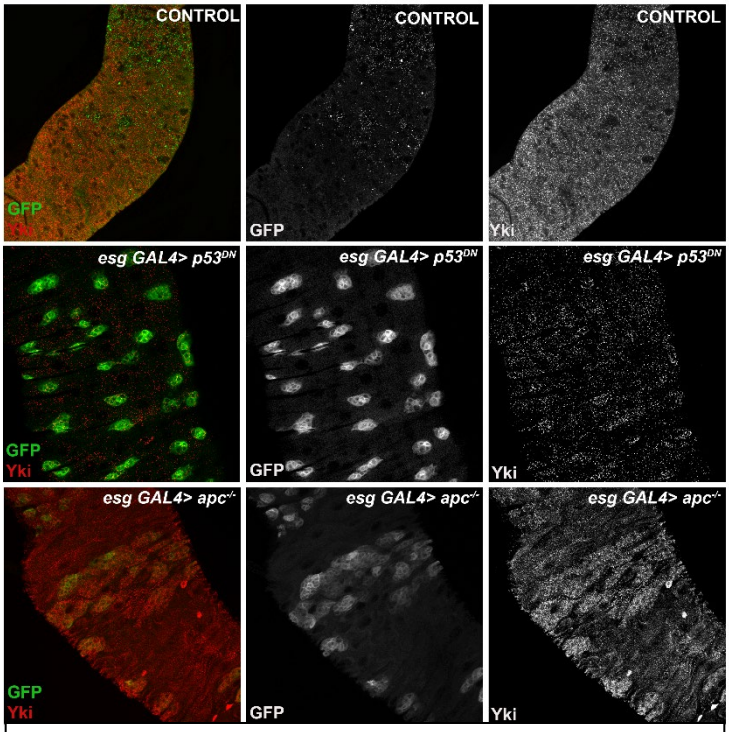

Figure 7: Panels show confocal images from (A) control, (B) *esgGAL4>UASp53^{DN}*, and (C) *esgGAL4>apc2,apc1*. The samples are stained with anti-Yki antibody (red, grey) and the GFP (green) marks the Gal4 driven tumor. All images are taken at 20X magnification, under identical settings for image acquisition on the confocal microscope.

Yki levels and localization in one-hit models: First, we tested the levels and localization of Yki, the Hippo pathway effector in our studies (Fig. 7). In the wild-type intestines (where no genes were manipulated), Yki is expressed in a punctate manner (Fig.

7 top row). In guts dissected from the *UASp53^{DN}* (Fig. 7 middle row) and *FRT82B apc2 apc1* (Fig. 7 bottom row) single-hit models, Yki expression is shown in red and grey. GFP expression is shown as green. The controls for these stocks were put through the same procedure as the experimental group, but without temperature treatment to activate the UAS/Gal4 and FLP/FRT systems. The control images show positive staining, but no oncogenesis or abnormal tissue structures (Fig. 7, top row). Stained cells are uniformly distributed and show no sign of damage. Middle B shows the effect of the experimental procedure on the *esgGal4>UASp53^{DN}* model. The first panel shows the result of GFP markers in green and anti-Yki staining in red. Multiple cell masses can be seen expressing the GFP markers that are evenly distributed across the hindgut. Masses all vary in both size and shape with jagged borders. The second and third panels show anti-Yki staining in grey. Masses are seen in the same location as the masses in panel one. Row C shows the effect of the experimental procedure on the *esgGal4/+; FRT82B Tub Gal80/ FRT82B apc2^{N175K} apc1^{Q8}* model. The tumor-clones are shown by GFP markers in green and anti-Yki markers in red. Multiple clones can be seen gathered in close proximity to each other in a band across the gut. Panels two and three show anti-Yki staining in grey. The clones appear to be large and smooth-edged suggesting homotypic sorting. Interestingly, high levels of Yki expression are seen in the tumor clones (Fig. 7 bottom row). Overall, these one-hit models reveal that Yki levels are not affected in all tested genotypes. Increased Yki levels in loss of apc genes suggests that these genes normally regulate Yki and ensure organ size and control of cell proliferation.

Wg levels and localization in one-hit models: Next, we tested the levels and localization of Wg, the Wingless pathway effector in our studies (Fig. 8). In the wild-type

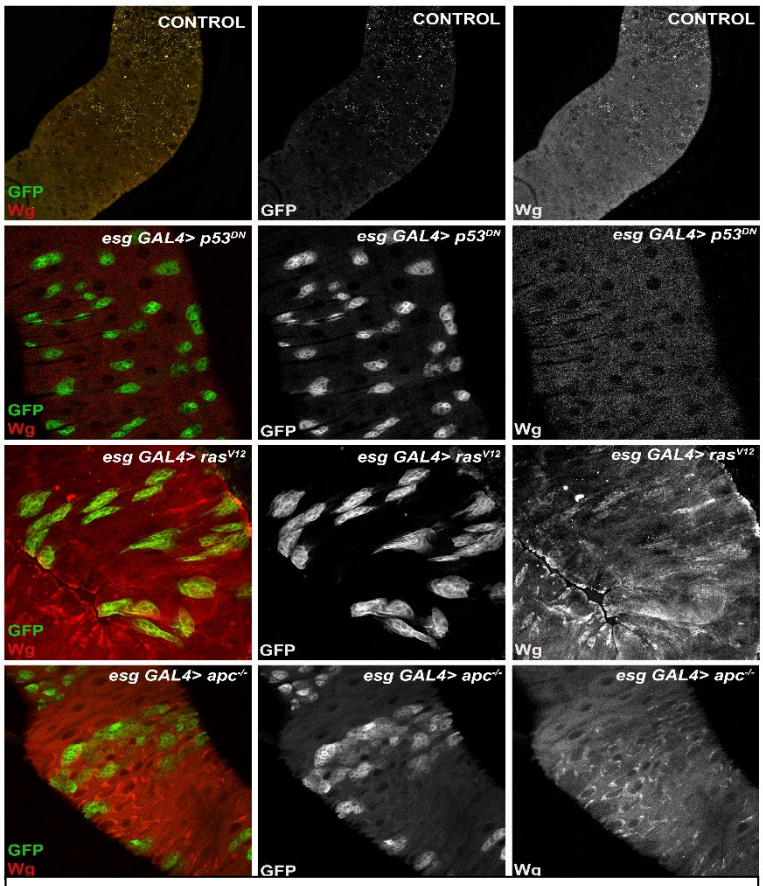

Figure 8: Panels show confocal images from (A) control, (B) *esgGAL4>UASp53*^{DN}, (C) *esgGal4>UASRas*^{V12}, and (D) *esgGAL4>apc2,apc1*. The samples are stained with anti-Wg antibody (red, grey) and the GFP (green) marks the Gal4 driven tumor. All images are taken at 20X magnification, under identical settings for image acquisition on the confocal microscope.

intestines, very little Wg was expressed (Fig. 8 top row). In hindguts dissected from the *UASp53*^{DN} (Fig. 8 row 2), *UASRas*^{V12} (Fig. 8 row 3), and *FRT82B apc2*^{N175K} *apc1*^{Q8} (Fig. 8 bottom row) single-hit models, Wg expression is shown in red (left column) and grey (right column). GFP expression is shown as green (left column) and grey (middle column). The controls for these stocks were put through the same procedure as the experimental group, but without temperature treatment to activate the UAS/Gal4 and FLP/FRT systems. The control images show positive staining, but no oncogenesis or abnormal tissue structures (Fig. 8, top row). Stained cells are uniformly distributed and show no sign of damage. Row 2 shows the effect of the experimental procedure on the *esgGal4>UASp53*^{DN} model. The first panel shows the result of the GFP marker in green and anti-Wg staining in red. Multiple cell masses can

be seen expressing the GFP that are evenly distributed across the hindgut. Masses all vary in both size and shape with jagged borders. The second and third panels show anti-Wg staining in grey. Masses are seen in the same location as the masses in panel one. Row C shows the effect of the experimental procedure on the *esgGal4>UASRas^{V12}* model. The tumor-clones are shown by GFP markers in green and anti-Wg markers in red. Multiple clones can be seen spread in a "C" shape across the hindgut, varying in size and elongated shape. The clone borders appear to be jagged as well. Panels two and three of row C show anti-Wg staining in grey. Clones are in the same location as the clones in panel one. Row D shows the effect of the experimental procedure on the *esgGal4/+; FRT82B Tub Gal80/ FRT82B apc2^{N175K} apc1^{Q8}* model. The tumor-clones are shown by GFP markers in green and anti-Wg markers in red. Multiple clones can be seen gathered in close proximity to each other in a band across the hindgut. Panels two and three show anti-Wg staining in grey. The clones appear to be large and smooth-edged suggesting homotypic sorting. Overall, pilot data shows Wg expression is induced in a patchy pattern in the *UASRas^{V12}* and *FRT82B apc2 apc1* mutant clones, but this pattern is not seen in *UASp53^{DN}* clones. Thus, some pathways like Ras-induced MAPK may promote tumor growth by inducing Wg as one of the downstream signals. We will further investigate this result to confirm the nature of Wg expression in the one-hit clones.

pJNK levels and localization in one-hit models: Next, we tested the levels and localization of pJNK, the JNK pathway effector in our studies (Fig. 8). In the wild-type intestines, small amounts of pJNK were expressed (Fig. 9 top row). In gut dissected from the *UASRas^{V12}* (Fig. 9 row 2), *UASp53^{DN}* (Fig. 9 row 3), and *FRT82B apc2^{N175K} apc1^{Q8}*

(Fig. 9 bottom row) single-hit models, pJNK activity is shown in red and grey. GFP expression is shown as green. The controls for these stocks were put through the same procedure as the experimental group, but without temperature treatment to activate the UAS/Gal4 and FLP/FRT systems. The control images show positive staining, but no oncogenesis or abnormal tissue structures (Fig. 9, top row). Stained cells are uniformly distributed and show no sign of damage. Row 2 shows the effect of the experimental procedure on the *esgGal4>UASRas^{V12}* model. The first panel shows the result of GFP markers in green and anti-pJNK staining in red. Multiple cell masses can be seen expressing the GFP markers that are evenly distributed across the gut. Masses all vary in both size and shape with jagged borders. The second and third panel shows pJNK

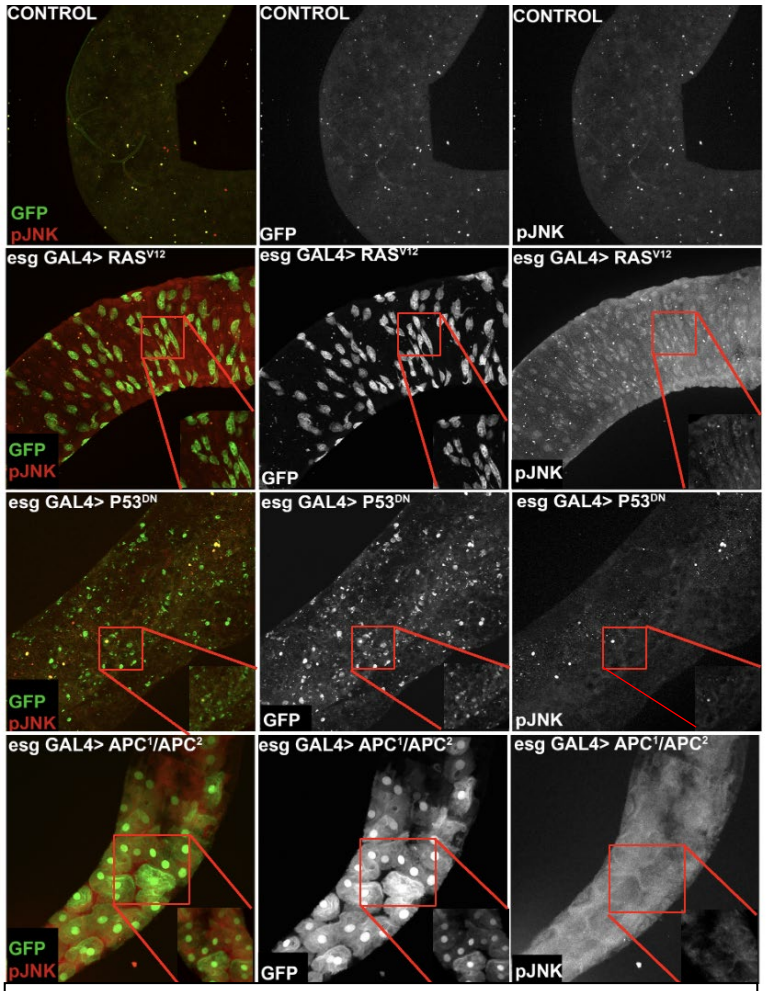

Figure 9: Panels show confocal images from (A) control, (B) esgGal4>Rasv12, (C) esgGAL4>p53DN, and (D) esgGAL4>apc2,apc1. The samples are stained with anti-pJNK antibody (red, grey) and the GFP (green) marks the Gal4 driven tumor. All images are taken at 20X magnification, under identical settings for image acquisition on the

activity in grey. pJNK is expressed in a majority of the clones. Row 3 shows the effect of the experimental procedure on the *esgGal4>UASp53^{DN}* model. The tumor-clones are shown by GFP markers in green and anti-pJNK markers in red. Multiple clones can be seen evenly spread across the hindgut with varying sizes and shapes with jagged edges. Panels two and three of row C show anti-pJNK staining in grey. pJNK expression is not seen in a majority of the clones. Row 4 shows the effect of the experimental procedure on the *esgGal4/+; FRT82B Tub Gal80/ FRT82B apc2^{N175K} apc1^{Q8}* model. The tumor-clones are shown by GFP markers in green and anti-pJNK markers in red. Panels two and three show anti-pJNK staining in grey. The clones appear to be large and smooth-edged, suggesting homotypic sorting. pJNK levels appear higher than wild type (Fig. 9, top row). Overall, these one-hit data reveal that all models do not induce pJNK, but it is induced in varying levels in the *UAS Ras^{V12}* and *apc2, apc1* clones. We will further confirm these observations by increasing our sample size and taking higher resolution and higher magnification images for these experiments.

Chapter 4

Discussion & Conclusions

These studies revealed that the markers for the Hippo, Wnt, and JNK pathways were highly expressed in the models and the rates of oncogenesis observed in the intestinal samples were higher than that in the wild-type control samples (Figures 7-9). Anti-Yki, Wg, and pJNK staining indicated that the single-hit models allowed for the generation and proliferation of cancerous cells along the hindgut. While each model was successful and the procedure was identical between them, the generated tumors varied from each other in size and shape. Tumor-clones generated from our $UASRas^{V12}$ model were larger than those of the $UASp53^{DN}$ or <*apc2, apc1*. Their shape was elongated and jagged. The tumors were observed to proliferate in both a spreading and crowding manner as visible in Figure 8. They covered a large region of the hindgut, but it was also observed that there were regions of no abnormal cell growth and other regions where the tumors crowded each other.

In contrast, tumor-clones generated from the $UASp53^{DN}$ model were very evenly distributed across the hindgut. Unlike the proliferation seen in the $UASRas^{V12}$ model, the tumor-clones from the $UASp53^{DN}$ model were observed to have consistent expression and oncogenesis throughout the sample. The tumors generated in this line varied in size as visible in Figures 7-9. While still smaller than those of the $UASRas^{V12}$ model, in Figures 7 and 8 they are observed to be nearly the same size while in Figure 9 they appeared much smaller, though with greater tumor proliferation across the intestine. The shape of the $UASp53^{DN}$ model was unique from the other single-hit models in that tumor-clones

generated from this model appeared less elongated and more spherical. The borders of these tumors were jagged, similar to the *UASRas*^{V12} model.

Lastly, the *<apc2, apc1* model showed different characteristics than that of the *UASp53*^{DN} and *UASRas*^{V12} models. The *<apc2, apc1* models generated tumor-clones similar in shape to that of the *UASRas*^{V12} model in that they are both elongated. The borders of these tumor-clones were observed to be smooth which is unique from the tumors seen in the other models. Tumors from this model also were observed to proliferate in close proximity to each other as visible in Figures 7 and 8. This is similar to the tumor behavior observed in the *UASRas*^{V12} model, though at a greater density. The overall size of the tumors in this model was observed to be between the size of those of the other models, though closer in size to those of the *UASRas*^{V12} model.

In both human and fly models, intestinal tumors proliferate in different ways due to a variety of factors such as genes involved or the environment (Mori, Yuichi, et al., 2016). This is further supported by the observed differences in tumor characteristics in our single-hit models. These variations in factors create the different tumors visible in Figure 10. Understanding the ways in which individual mutations contribute to the

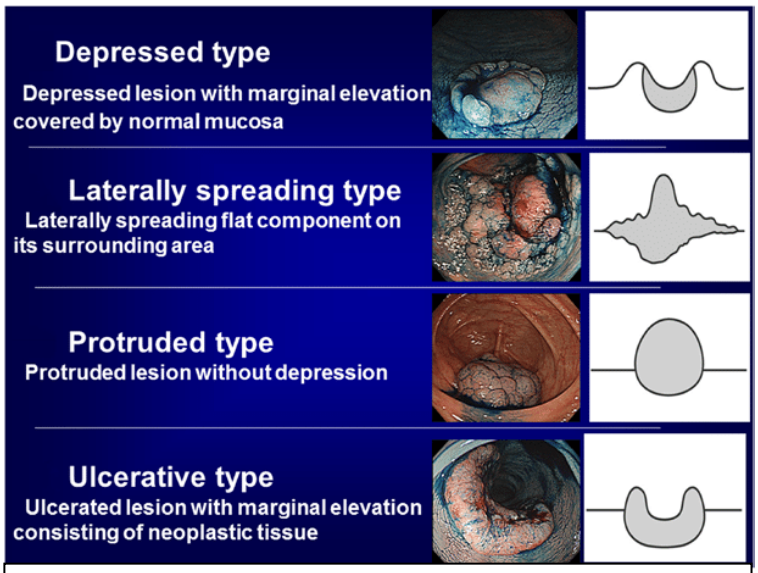

Figure 10: Pictures portraying some of the different shapes CRC tumors proliferate into in humans. (Mori, Yuichi et al., 2016)

development and proliferation of tumors helps us not only better understand the ways in which these different cellular pathways interact but also to help determine the prognosis of each unique CRC case. The pilot data collected from this experiment shows potential for developing this necessary understanding. Further research and observations need to be done in order to confirm the reliability of our models as well as how these individual mutations contribute to cooperative oncogenesis. The development of our three-hit model will help us towards this goal.

Future Directions

In the future, I would like to see how target medicine can be used in combination with this research to treat the cancer developed in our models. This could include supplementing the models with properly functioning proteins or experimenting with knockout treatments for oncogenes. I plan to continue this research to generate two-hit models as well so the relationship between the different pathways can be better understood.

References

Armaghany, Tannaz, Jon D. Wilson, Quyen Chu, and Glenn Mills. "Genetic Alterations in Colorectal Cancer." *Gastrointestinal Cancer Research: GCR* 5, no. 1 (January 2012): 19–27.

Barwell, Taylor, Sofia Geld, and Laurent Seroude. "Comparison of GAL80ts and Tet-off GAL80 Transgenes." *microPublication Biology* 2023 (2023). https://doi.org/10.17912/micropub.biology.000770.

Bejsovec, A. (2018). Wingless Signaling: A Genetic Journey from Morphogenesis to Metastasis. *Genetics* **208**, 1311–1336.

Brand, A. H. and Perrimon, N. (1993). Targeted gene expression as a means of altering cell fates and generating dominant phenotypes. *Development* **118**, 401–415.

Brumby, Anthony M., and Helena E. Richardson. "Using Drosophila *Melanogaster* to Map Human Cancer Pathways." *Nature Reviews Cancer* 5, no. 8 (August 1, 2005): 626–39. https://doi.org/10.1038/nrc1671.

Caygill, E. E. and Brand, A. H. (2016). The GAL4 System: A Versatile System for the Manipulation and Analysis of Gene Expression. In *Drosophila* (ed. Dahmann, C.), pp. 33–52. New York, NY: Springer New York.

Centers for Disease Control and Prevention. (2023, February 23). *What should I know about screening for colorectal cancer?* Colorectal (Colon) Cancer. https://www.cdc.gov/cancer/colorectal/basic_info/screening/index.htm#:~:text=Screening%20Recommendations&text=The%20Task%20Force%20recommends%20several,Learn%20about%20these%20screening%20tests.

***Colon cancer: American Cancer fund*®.** American Cancer Fund® | Official Site of the American Cancer Fund®. (2021, August 6). https://americancancerfund.org/cancer-types/colon-cancer/

Dillard, Caroline, José Gerardo Teles Reis, and Tor Erik Rusten. "RasV12; Scrib-/- Tumors: A Cooperative Oncogenesis Model Fueled by Tumor/Host Interactions." *International Journal of Molecular Sciences* 22, no. 16 (August 18, 2021): 8873. https://doi.org/10.3390/ijms22168873.

Delaval, B. and Birnbaum, D. (2007). A cell cycle hypothesis of cooperative oncogenesis (Review). *Int J Oncol*.

Dillard, C., Reis, J. G. T. and Rusten, T. E. (2021). RasV12; scrib−/− Tumors: A Cooperative Oncogenesis Model Fueled by Tumor/Host Interactions. *IJMS* **22**, 8873.

Doggett, Karen, Felix A. Grusche, Helena E. Richardson, and Anthony M. Brumby. "Loss of the Drosophila Cell Polarity Regulator Scribbled Promotes Epithelial Tissue Overgrowth and Cooperation with Oncogenic Ras-Raf through Impaired Hippo Pathway Signaling." *BMC Developmental Biology* 11 (September 29, 2011): 57. https://doi.org/10.1186/1471-213X-11-57.

Germani, Federico, Cora Bergantinos, and Laura A Johnston. "Mosaic Analysis in *Drosophila*." *Genetics* 208, no. 2 (February 1, 2018): 473–90. https://doi.org/10.1534/genetics.117.300256.

Islam, Md Rezaul, Shopnil Akash, Md Mominur Rahman, Feana Tasmim Nowrin, Tamanna Akter, Sheikh Shohag, Abdur Rauf, Abdullah S.M. Aljohani, and Jesus Simal-Gandara. "Colon Cancer and Colorectal Cancer: Prevention and Treatment by Potential Natural Products." *Chemico-Biological Interactions* 368 (December 2022): 110170. https://doi.org/10.1016/j.cbi.2022.110170.

Jennings, B. H. (2011). Drosophila – a versatile model in biology & medicine. *Materials Today* **14**, 190–195.

Johnson, R. and Cagan, R. (2010). Drosophila as a Model for Human Disease. In *Vogel and Motulsky's Human Genetics* (ed. Speicher, M. R.), Motulsky, A. G.), and Antonarakis, S. E.), pp. 795–811. Berlin, Heidelberg: Springer Berlin Heidelberg.

Kango-Singh, M. and Singh, A. (2009). Regulation of organ size: Insights from the *Drosophila* Hippo signaling pathway. *Developmental Dynamics* **238**, 1627–1637.

Kim, Minseong, and Eek-Hoon Jho. "Cross-Talk between Wnt/β-Catenin and Hippo Signaling Pathways: A Brief Review." *BMB Reports* 47, no. 10 (October 2014): 540–45. https://doi.org/10.5483/bmbrep.2014.47.10.177.

La Marca, J. E. and Richardson, H. E. (2020). Two-Faced: Roles of JNK Signalling During Tumourigenesis in the Drosophila Model. *Front. Cell Dev. Biol.* **8**, 42.

Lee, T. and Luo, L. (1999). Mosaic Analysis with a Repressible Cell Marker for Studies of Gene Function in Neuronal Morphogenesis. *Neuron* **22**, 451–461.

Ma, Xianjue, Yujun Chen, Wenyan Xu, Nana Wu, Maoquan Li, Ying Cao, Shian Wu, Qiutang Li, and Lei Xue. "Impaired Hippo Signaling Promotes Rho1–JNK-Dependent Growth." *Proceedings of the National Academy of Sciences* 112, no. 4 (January 27, 2015): 1065–70. https://doi.org/10.1073/pnas.1415020112.

McGuire, S. E., Mao, Z. and Davis, R. L. (2004). Spatiotemporal Gene Expression Targeting with the TARGET and Gene-Switch Systems in *Drosophila*. *Sci. STKE* **2004**,.

Mirzoyan, Z., Sollazzo, M., Allocca, M., Valenza, A. M., Grifoni, D. and Bellosta, P. (2019). Drosophila melanogaster: A Model Organism to Study Cancer. *Front. Genet.* **10**, 51.

Mori, Yuichi, Shin-Ei Kudo, Shungo Endo, Chiyo Maeda, Shumpei Mukai, Yasuharu Maeda, Shinichi Kataoka, et al. "Morphology as a Risk Factor for the Malignant Potential of T2 Colorectal Cancer." *Molecular and Clinical Oncology* 5, no. 3 (September 2016): 223–26. https://doi.org/10.3892/mco.2016.951.

Nakayama, Mizuho, and Masanobu Oshima. "Mutant *P53* in Colon Cancer." *Journal of Molecular Cell Biology* 11, no. 4 (April 1, 2019): 267–76. https://doi.org/10.1093/jmcb/mjy075.

Nouri Nojadeh, Jafar, Shahin Behrouz Sharif, and Ebrahim Sakhinia. "Microsatellite Instability in Colorectal Cancer." *EXCLI Journal; 17:Doc159; ISSN 1611-2156*, 2018. https://doi.org/10.17179/EXCLI2017-948.

Parnell, R. W. "Weight Penalties." *British Medical Journal* 2, no. 6202 (December 1, 1979): 1441. https://doi.org/10.1136/bmj.2.6202.1441.

Reddy, Sujana. "Physiology, Circadian Rhythm," n.d.

Schatoff, Emma M., Benjamin I. Leach, and Lukas E. Dow. "Wnt Signaling and Colorectal Cancer." *Current Colorectal Cancer Reports* 13, no. 2 (April 2017): 101–10. https://doi.org/10.1007/s11888-017-0354-9.

Richardson, H. E., Cordero, J. B. and Grifoni, D. (2020). Basic and Translational Models of Cooperative Oncogenesis. *IJMS* **21**, 5919.

Sanchez-Vega, F., Mina, M., Armenia, J., Chatila, W. K., Luna, A., La, K. C., Dimitriadoy, S., Liu, D. L., Kantheti, H. S., Saghafinia, S., et al. (2018). Oncogenic Signaling Pathways in The Cancer Genome Atlas. *Cell* **173**, 321-337.e10.

Snigdha, K., Gangwani, K. S., Lapalikar, G. V., Singh, A. and Kango-Singh, M. (2019). Hippo Signaling in Cancer: Lessons From Drosophila Models. *Front. Cell Dev. Biol.* **7**, 85.

Sun, Gongping, and Kenneth D. Irvine. "Regulation of Hippo Signaling by Jun Kinase Signaling during Compensatory Cell Proliferation and Regeneration, and in Neoplastic Tumors." *Developmental Biology* 350, no. 1 (February 2011): 139–51. https://doi.org/10.1016/j.ydbio.2010.11.036.

Valle Rodríguez, Alberto del, Dominic Didiano, and Claude Desplan. "Power Tools for Gene Expression and Clonal Analysis in Drosophila." *Nature Methods* 9, no. 1 (December 28, 2011): 47–55. https://doi.org/10.1038/nmeth.1800.

Vanderstraeten, Jacques, Philippe Gailly, and E. Pascal Malkemper. "Light Entrainment of Retinal Biorhythms: Cryptochrome 2 as Candidate Photoreceptor in Mammals." *Cellular and Molecular Life Sciences* 77, no. 5 (March 2020): 875–84. https://doi.org/10.1007/s00018-020-03463-5.

Waghmare, I., Roebke, A., Minata, M., Kango-Singh, M. and Nakano, I. (2014). Intercellular Cooperation and Competition in Brain Cancers: Lessons From Drosophila and Human Studies. *Stem Cells Translational Medicine* **3**,.

Waghmare, I., Gangwani, K., Rai, A., Singh, A. and Kango-Singh, M. (2023). *A Tumour-Specific Molecular Network Promotes Tumour Growth in* Drosophila *by Enforcing a JNK-YKI Feedforward Loop*. Cancer Biology.

Yasuta, Y., Kaminaka, R., Nagai, S., Mouri, S., Ishida, K., Tanaka, A., Zhou, Y., Sakurai, H. and Yokoyama, S. (2024). Cooperative function of oncogenic MAPK signaling and the loss of Pten for melanoma migration through the formation of lamellipodia. *Sci Rep* **14**, 1525.